Check for
updates

CMOS-MEMS Vibro-Impact Devices and Applications

*Chun-Pu Tsai and Wei-Chang Li**

Resonant MEMS Laboratory (Resolab), Institute of Applied Mechanics, National Taiwan University, Taipei, Taiwan

CMOS-MEMS-based vibro-impact devices that utilize impact-induced nonlinear dynamics have been shown to yield unique and unprecedented functionalities with on-chip integration capability. For example, a 0.35-µm CMOS-based capacitively transduced comb-driven folded-beam resonant switch has been integrated with backend circuits to demonstrate a zero-quiescent power wireless receiver operating at the low-frequency (LF) band. In addition, CMOS-MEMS vibro-impact resonators have been used as AFM-alike surface condition monitoring for detecting chemical coating on structural sidewalls and clock generators with controllable duty cycles by manipulating the actuation conditions. This article will review these achievements and discuss the limitations and challenges in developing the vibro-impact devices using the CMOS-MEMS technology.

Keywords: vibro-impact resonator, resoswitch, CMOS-MEMS, nonlinear dynamics, impact nonlinearity

1 INTRODUCTION

Vibro-impact systems, referring to regular vibration systems with displacement stoppers that physically constrain the vibration magnitude and, in turn, cause periodic collisions to occur, have been widely studied for machine dynamics and vibration engineering (Babitsky, 2013; Luo and Guo, 2013). Such collisions may result in loose joints, noise, and even failure in machines and are generally not welcome. However, they could become rather useful in some cases. Drilling machines, vibro-impact hammers, and pile drivers serve as excellent examples of constructive usages of impact dynamics. Interestingly, MEMS technology that can realize mechanical structures and devices on the microscopic scale also encompasses the pros and cons of impact dynamics. For example, numerous studies focus on characterizing and eliminating contact bounces of MEMS switches (Patton and Zabinski, 2005; Peschot, 2014), whereas others use impact-induced dynamics to build useful devices and tools such as impact energy harvesters (Moss, 2010; Yang, 2014; Fu, 2018; Dauksevicius, 2019), tapping mode resonators (Zhang et al., 2005; He et al., 2014; Riverola et al., 2016), and atomic force microscopy (Lee et al., 2002; Hölscher, 2012).

On the other hand, recent advances in CMOS-MEMS fabrication process platforms have enabled extensive research activities and demonstrations of making miniaturized sensors and actuators in CMOS with inherent monolithic circuit integration and fast concept prototyping capabilities. Examples include chemical/environmental sensors (Xu, 2016; Lee, 2021a; Lee, 2021b), inertial sensors (Luo et al., 2002; Xie and Fedder, 2003; Wu et al., 2004; Sun et al., 2010; Chiu et al., 2013), and resonant components (Lo et al., 2005; Verd 2005; Verd, 2008; Chen et al., 2011; Li et al., 2016; Galanko, 2017). Similarly, CMOS-MEMS platforms also allow the implementation of miniaturized vibro-impact devices. For example, Lu et al. (2018a) demonstrate the first CMOS-MEMS resoswitches based on a CMOS-MEMS clamped–clamped beam (CC-beam) resonator. Meanwhile, with continuous efforts invested in process improvement (Dai, 2006;

FIGURE 1 | CMOS-MEMS relays and resoswitches. **(A)** SEM and schematic of CMOS-MEMS tungsten VIA cantilever relay of Riverola et al. (2014). **(B)** Tungsten and aluminum stacking CC-beam resoswitch of Lu et al. (2018a). Reproduced from Riverola et al. (2014) and Lu et al. (2018a) with permission from IEEE.

FIGURE 2 | Illustration of the oxide layer after release if the VIA wall is allowed or not. **(A)** The CMOS-MEMS process used in Lu et al. (2018a), where the tungsten VIA is allowed to have a continuous "wall" to protect the enclosed intermediate oxide from being etched by the release etchant. **(B)** If VIA "wall" is not allowed.

Hsu and Li, 2020), the CMOS-MEMS platforms are not only used to repeat what has been done in non-CMOS platforms but also, like the later cases based on CMOS-MEMS vibro-impact resonators, allow innovations of unique devices and applications.
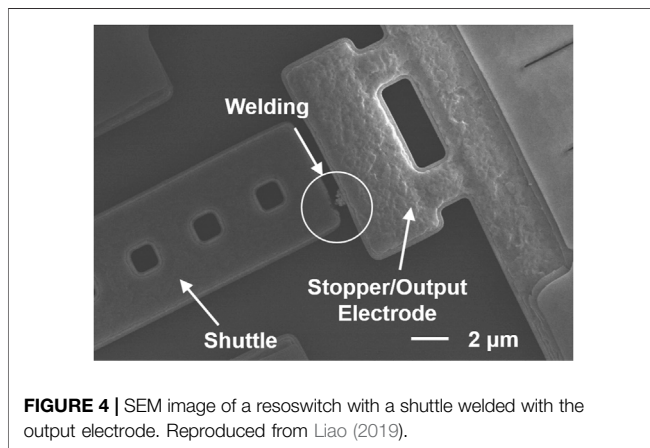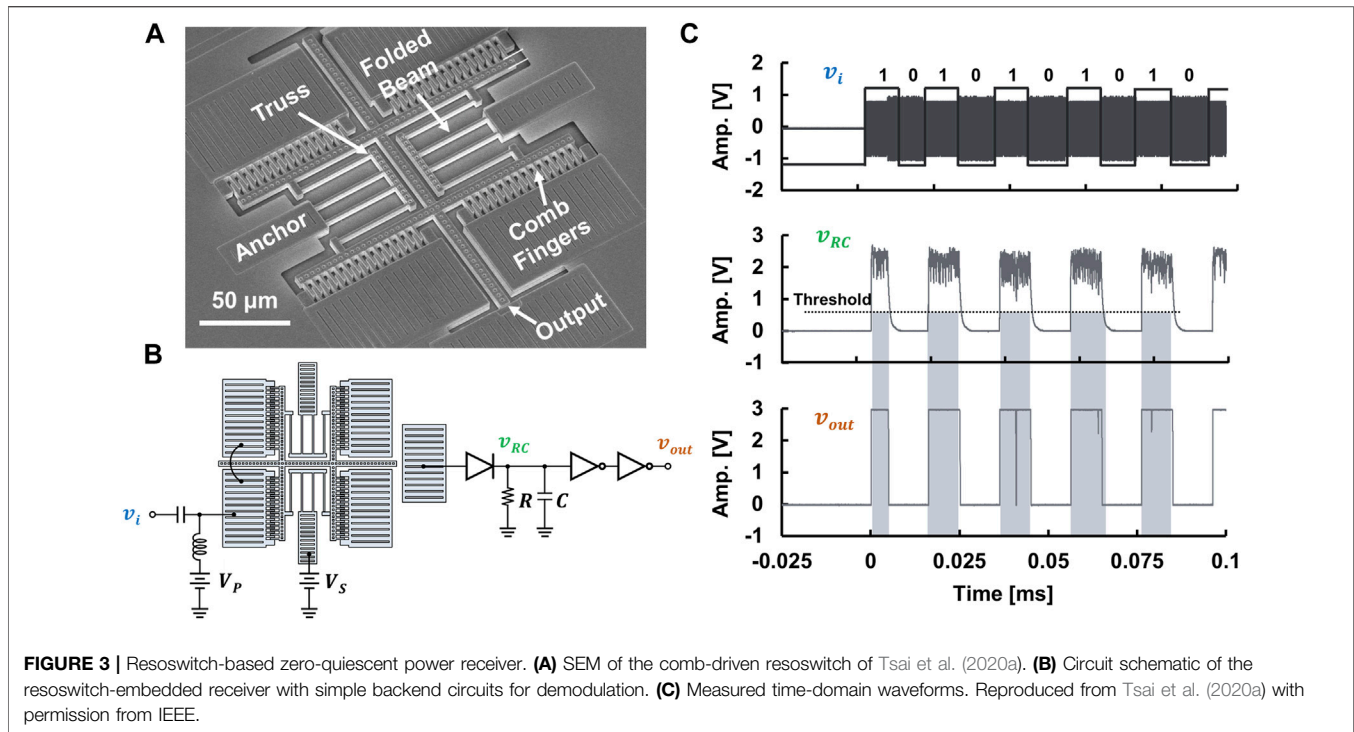
This article will first discuss the vibro-impact resoswitch development, which would be a MEMS technology most relevant to vibro-impact resonators. Then, the process, development, and limitations of CMOS-MEMS vibro-impact resonators will be reviewed in **Section 2**. Next, CMOS-MEMS vibro-impact device-derived zero-quiescent power receiver,

surface condition monitoring, and nonlinear dynamic applications will be summarized in **Sections 3–5**. Through the discussion, design considerations and challenges for each of the applications will be addressed. **Section 6** finally concludes this article.

1.1 Resoswitch Evolvement

Before proceeding to CMOS-MEMS vibro-impact devices and applications, it is instructive to first discuss the development of MEMS resonant switches ("resoswitches"). The research activities of MEMS vibro-impact resonators can be tracked back to MEMS resoswitches. Resoswitches were originally proposed in Lin et al. (2008) to tackle the issues of high actuation voltage, slow switching speed, and poor reliability in conventional MEMS switches via resonance operation, at which the switching frequency and restoring force would be increased while the required driving voltage could be reduced due to the larger displacement magnitude compared to that at static state.

The first MEMS resoswitch resonator of Lin et al. (2008) was based on a wine-glass-mode disk resonator. Such a resonator has identical vibration amplitudes along the input and output axes, which cause impacts to occur not only at the output but also at the input electrode. The short circuit between the input and the resonator structure would affect the driving signal integrity and even device failure due to the usual higher voltage drop across compared to that between the disk and the output. To mitigate this, displacement amplification between the driving and the output axes becomes necessary. Kim (2009), Lin (2009), and Li et al. (2016) used either structural modification or geometrical design to yield unbalanced stiffness along the input and the

FIGURE 3 | Resoswitch-based zero-quiescent power receiver. **(A)** SEM of the comb-driven resoswitch of Tsai et al. (2020a). **(B)** Circuit schematic of the resoswitch-embedded receiver with simple backend circuits for demodulation. **(C)** Measured time-domain waveforms. Reproduced from Tsai et al. (2020a) with permission from IEEE.

FIGURE 4 | SEM image of a resoswitch with a shuttle welded with the output electrode. Reproduced from Liao (2019).

output and in turn displacement amplification between the two ports. On the other hand, while a power amplification (not voltage amplification) was still achievable using the devices listed above, their polysilicon material exhibited a higher contact resistance on the order of tens of kΩ to MΩ range, greatly hindering the power transmit applications. Later, metal started to replace polysilicon and became the structure/surface material. Lin (2011) presented the first metal resoswitch using electroplated Ni followed by the one using metal Al of Li et al. (2013) and Au of Liu (2015). Alternatively, heterogeneous approaches that modify the contact surfaces of polysilicon or AlN resonator structures with metal Pt (Wu, 2017), W (Liu et al., 2017), Ru (Lin et al., 2013; Lin et al., 2013), Pt-silicide (Lin et al., 2014), or Ru-silicide (Liu et al., 2016) have been demonstrated.
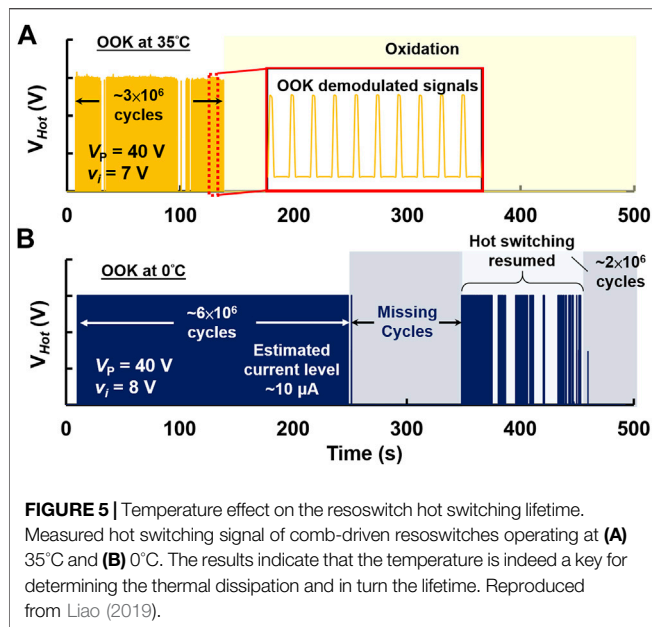
2 CMOS-MEMS VIBRO-IMPACT RESONATORS

In contrast to the demonstrations above, for which the fabrication processes were designed and tweaked specifically for each device, standard CMOS processes have also been used as a generic fabrication platform in making resoswitches. Differing from regular resonator devices, resoswitches require conductive surfaces for electrical connection at the mechanical contacts during operation.

2.1 CMOS-MEMS Fabrication Platforms
Typical CMOS-MEMS processes use metal, metal-oxide composite, or polysilicon layers for the structural materials, which leave metal (Lopez et al., 2009; Chen et al., 2011), oxide (Fedder, 1996; Liu, 2013), a mixture of metal and oxide, or polysilicon (Marigo, 2010) on the surfaces of resonator structures and electrodes. For switch applications, however, the metal version would be preferred, for which the release step that removes sacrificial oxide typically uses HF-based solution (Silox Vapox III by Transene Company, Inc.) with better selectivity against metal aluminum compared to regular HF or BHF.

2.2 CMOS-MEMS Relays and Resoswitches
Riverola (2014) presents a CMOS-MEMS-based mechanical switch, i.e., a relay, whose structure uses one of the VIA tungsten layers in a 0.35-μm CMOS process. **Figure 1A** presents the cross-section and SEM image of a fabricated CMOS-MEMS relay. The CMOS-MEMS platform also yields other relay devices, including Riverola et al. (2016) and Riverola et al. (2018). On the other hand, Lu et al. (2018a)

FIGURE 5 | Temperature effect on the resoswitch hot switching lifetime. Measured hot switching signal of comb-driven resoswitches operating at **(A)** 35°C and **(B)** 0°C. The results indicate that the temperature is indeed a key for determining the thermal dissipation and in turn the lifetime. Reproduced from Liao (2019).

demonstrate a CC-beam CMOS-MEMS resoswitch based on another 0.35-μm metal process (Liu et al., 2018) (*cf.* **Figure 1B**), in which multiple stacking layers are used instead. Compared to Riverola (2014), the resoswitch of Lu et al. (2018a) yields much lower contact resistances and in turn successful hot switching around 2 MHz. Tsai et al. (2020a) present another CMOS-MEMS-based resoswitch that uses a comb-driven folded-beam resonator. The comb-driven resoswitch targets the 125-kHz low-frequency (LF) band typically used for RFID systems. The latter two CMOS-MEMS resoswitches are based on a 0.35-μm 2-poly-4-metal (2P4M) CMOS process, for which special permission is granted by the foundry to allow continuous VIA layout. Therefore, the intermediate oxide can be protected by the surrounding VIA against the HF solution. **Figure 2A** illustrates how the continuous VIA "wall" protects the intermediate oxide in comparison to the case of **Figure 2B** if it is not allowed, where a VIA array would be used to bind each pair of metal layers. According to the authors' experience, such sparse VIAs might not adhere well to the metal layers once the surrounding oxide is released.

2.3 Limitations of CMOS-MEMS Platforms for Relay/Resoswitch Applications

Given the design rules and material CMOS-MEMS processes, the output gap spacing of resoswitches must obey the minimum spacing between metals. For instance, the comb-driven resoswitch of Tsai et al. (2020a) has a gap spacing of 0.6 μm between the shuttle and the output electrode. In addition, the options for contact materials are limited, for example, Al and W for the 0.35 μm CMOS used in Lu et al. (2018a) and W for Riverola et al. (2014). In other words, while offering a generic platform, CMOS-MEMS would suffer a bit of flexibility. It would be difficult to adopt specific contact materials preferred for MEMS switches (Ma, 2007).

3 CMOS-MEMS-BASED ZERO-QUIESCENT RF RECEIVERS

While the CMOS-MEMS relays aim to deliver better switches than the MOS version, the major applications of CMOS-MEMS resoswitches target particularly at the zero-quiescent power RF signal reception. Based on the comb-driven resoswitches, Tsai et al. (2020a) demonstrate signal reception and demodulation for FSK and OOK schemes at a 125-kHz low-frequency (LF) band. **Figure 3A** shows the SEM photo of the comb-driven resoswitches, and **Figure 3B** depicts the associated circuits for demodulation, which essentially comprise an *RC* filter with two cascaded inverters as a comparator to sharpen the digital bit transition. **Figure 3C** plots the FSK driving signal v_i, for which f_1 and f_2 are in- and out-of-resonance frequencies, respectively, applied to the resoswitch of **Figure 3B** and the corresponding signals at v_{RC} and v_{out}, demonstrating the capability of signal filtering, amplification, and demodulation, all done by the resoswitch embedded circuit of **Figure 3B**. More importantly, the circuit drops to zero power while listening to the incoming signal.
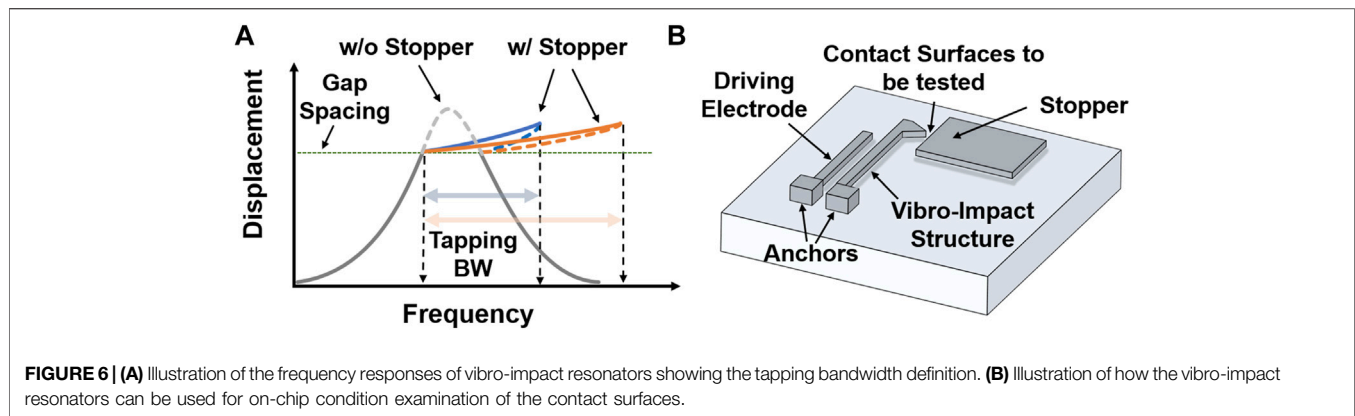
3.1 Sensitivity Improvement

Compared to non-CMOS or even electronic wake-up receivers, the RF reception sensitivity performance for resoswitch-based receivers greatly depends upon the characteristics of the resoswitch used. For the demonstration of **Figure 3C**, although a later work that used an off-chip transformer to boost the voltage gain and in turn used a 123-mV$_{PP}$ driving signal instead, the sensitivity level still has great room for improvement. For example, commercial LF wake-up receivers typically require a much smaller driving level on the order of 1 mV$_{PP}$ (Atmel, 2007; Austriamicrosystems, 2015).

To enhance sensitivity, transducer gap reduction would be one of the most effective ways to achieve so for capacitively-transduced MEMS resonators. Approaches for non-CMOS counterparts could be either adding materials, such as atomic-layer-deposition (ALD) (Akgul, 2009), to partially refill the gap or mechanically displace the structures via, for example, bistable snap-through (Pyatishev, 2017), after fabrication. Similarly, for CMOS resonant devices, the post-process mechanical approach has been demonstrated, including using electrostatic force (Chen et al., 2012) and intrinsic stress-induced deformation (Zheng et al., 2022) to pull the structure closer to the electrode. Of course, the gap-refilling technique might be applicable in CMOS technology. However, for the resoswitch application, while non-conductive refilling material is not suitable for electrical contact, an alternative process design and/or techniques will be necessary to apply conductive refilling materials only at the contact surfaces. Otherwise, the device I/O may be electrically shorted if the materials are deposited uniformly across the structure.

Although not finished yet, by combining the gap narrowing with *Q* enhancement techniques, CMOS-MEMS resoswitch-based receivers can be expected to achieve similar sensitivity levels as commercial ICs.

FIGURE 6 | (A) Illustration of the frequency responses of vibro-impact resonators showing the tapping bandwidth definition. **(B)** Illustration of how the vibro-impact resonators can be used for on-chip condition examination of the contact surfaces.

3.2 Resoswitch Reliability

As mentioned above, resoswitches were proposed to mitigate the issues of conventional MEMS switches. Nevertheless, the fundamental limitations of material handling electrical current flow follow the same physics as the conventional counterparts. As observed in countless experiments conducted here, the failure modes of resoswitches fall into two categories: surface oxidation and welding, both of which are governed by thermal management. **Figure 4** shows the SEM photo of a resoswitch whose shuttle and the output electrode are welded due to excessive power during hot switching (Liao, 2019). The contact handles an overall ~0.5 μW on average during hot switching assuming a contact resistance of 1 kΩ (Lu et al., 2018a). Although the structure tip is designed to be a few μm wide, the actual contact area might fall in a few tiny tips due to surface roughness. **Figure 5** compares the effect of operating temperature on the cycle counts. **Figures 5A, and B** plot the switching signal when operating the device at 35 and 0°C, respectively, showing that the operation at low temperature would improve switch reliability and facilitate switching recovery (postulated due to oxide breakage). The results identify the effect of temperature on contact reliability. While contact materials might not be applied flexibly in CMOS-MEMS platforms, proper thermal management via structural and packaging design would be key toward system integration **Figure 6**.

4 SURFACE CONDITION MONITORING

The frequency responses for vibro-impact resonators, i.e., referring to the cases with non-conductive contact surfaces, exhibit a tapping region with a tapping bandwidth dictated by the interaction force between the contact surfaces (*cf.* **Figure 6A**). The interaction forces include mechanical contact force, van der Waals forces, capillary forces, chemical bonding, electrostatic forces, Casimir forces, solvation forces, etc., all of which are functions of various parameters including temperature, contact material, structural stiffness, surface energy, and contact area. The tapping-mode atomic-force-microscopy (AFM) serves as an exact example of using these impact dynamics and

interaction forces to measure the properties of object surfaces. **Figure 6B** illustrates that a vibro-impact resonator could be used as an "on-chip" AFM whose frequency response can reflect the contact surface condition.

Lu et al. (2018b) showed the influence of surface chemical coating on the tapping frequency responses of vibro-impact resonators. Applying (1H, 1H, 2H, 2H)-perfluorodecyltrichlorosilane (FDTS) chemical to a CMOS-MEMS CC-beam vibro-impact resonator yields a wider tapping bandwidth due to the reduced surface energy. **Figure 7** illustrates the salinization process, in which a die with vibro-impact resonators is placed in a vacuum jar together with a 20-μl FDTS followed by vaporizing FDTS via pumping. Then, the pump is turned off and the vaporized FDTS is allowed to settle and coat the device surface. A test sample with blank aluminum, showing a hydrophobic surface after salinization, verifies the process flow. The measured frequency responses under tapping operation reveal the change of tapping bandwidth from 17.37 kHz before FDTS to 29.75 kHz after FDTS coating. This effect can be used to perform on-chip surface condition monitoring for chemical coating in applications such as MEMS inertial sensors. In this work of Lu et al. (2018b), the contact model borrowing that from Derjaguin et al. (1975) uses the Hamaker constant to define the van der Waals body–body interaction at contact.

5 NONLINEAR DYNAMICS

Vibro-impact systems undergo nonlinear dynamics induced by both mechanical nonlinearity and impact (Rhoads et al., 2010). The derivations of the dynamic model greatly benefit from that of atomic force microscopy (Lee et al., 2002). However, the merged nonlinearity of vibro-impact resonators presents unique characteristics and allows more applications beyond the AFM-like feature presented in **Section 4**. For example, operating the devices at the impact-induced bifurcation points would yield better frequency stability. In addition, by controlling the driving conditions, vibro-impact resonators would exhibit variable bifurcation behaviors, among which the period-doubling
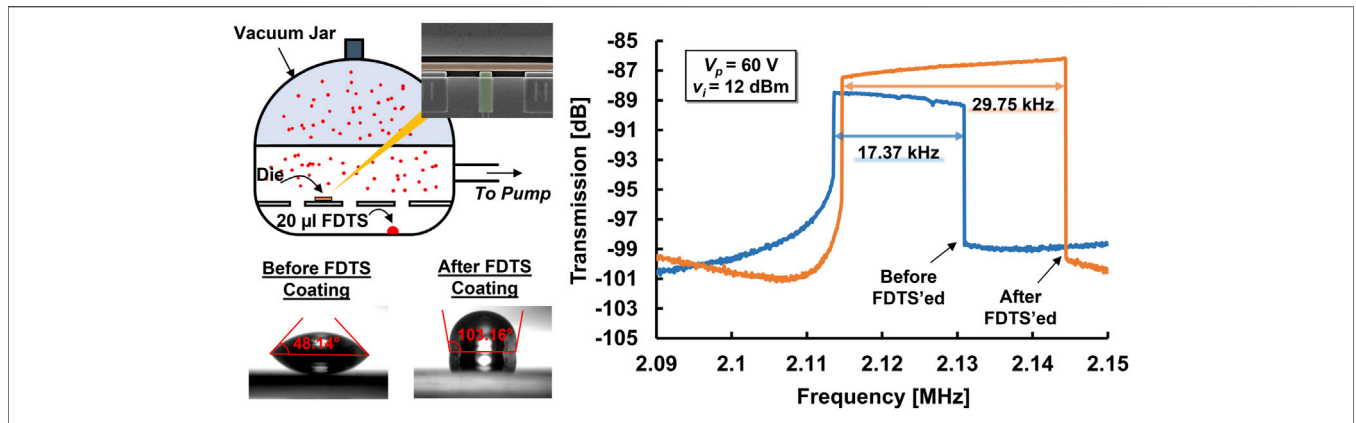
FIGURE 7 | A CC-beam vibro-impact resonator is used to study the tapping responses under the influence of surface coating with FDTS chemicals. Reproduced from Lu et al. (2018b) with permission from IEEE.
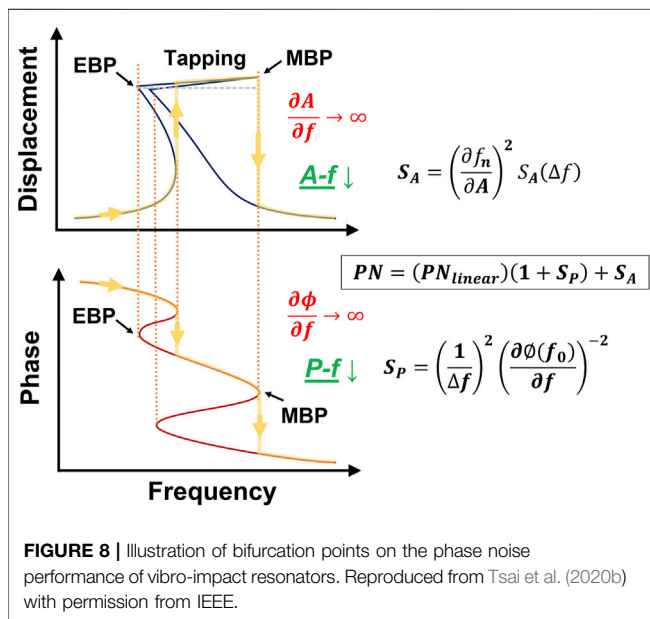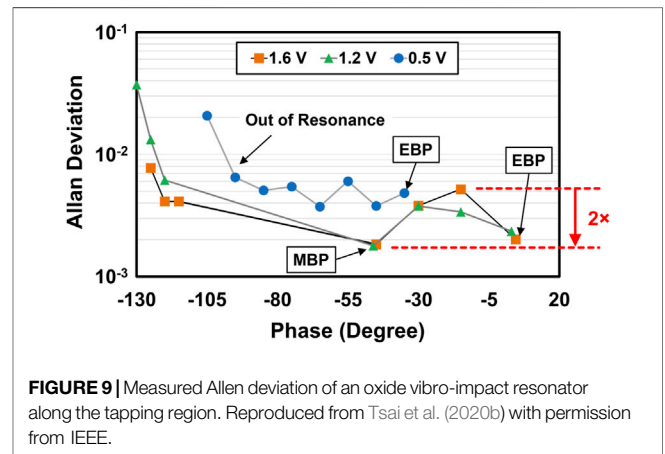

FIGURE 8 | Illustration of bifurcation points on the phase noise performance of vibro-impact resonators. Reproduced from Tsai et al. (2020b) with permission from IEEE.

FIGURE 9 | Measured Allen deviation of an oxide vibro-impact resonator along the tapping region. Reproduced from Tsai et al. (2020b) with permission from IEEE.

frequency, regular frequency sweeping would exhibit discontinuous curves and some part of the transmission cannot be reached. The light yellow curves in **Figure 8** illustrate forward sweeping responses. On the other hand, the phase-to-frequency relation is rather one to one, meaning a phase value corresponds to only a single frequency. This allows one to use phase locked loop circuits to obtain the complete frequency responses. Along the tapping region, the left and right ends represent two bifurcation points: electrical bifurcation point (EBP) and mechanical bifurcation point (MBP), respectively. These points exhibit infinite slopes of amplitude-to-frequency and phase-to-frequency. According to the nonlinear phase noise, it can achieve a minimum when the two effects have infinite slopes.

Tsai et al. (2020b) reported the Allan deviations for a CMOS-MEMS oxide vibro-impact CC-beam resonator operating around the tapping region. As shown in **Figure 9** and the theory predicts, the EBP and MBP yield lower Allan deviations when connected to oscillators compared to other points on the tapping flat region, verifying that the bifurcation points indeed have strong influences on the frequency stability.

bifurcation can be utilized to achieve various switching duty cycles.
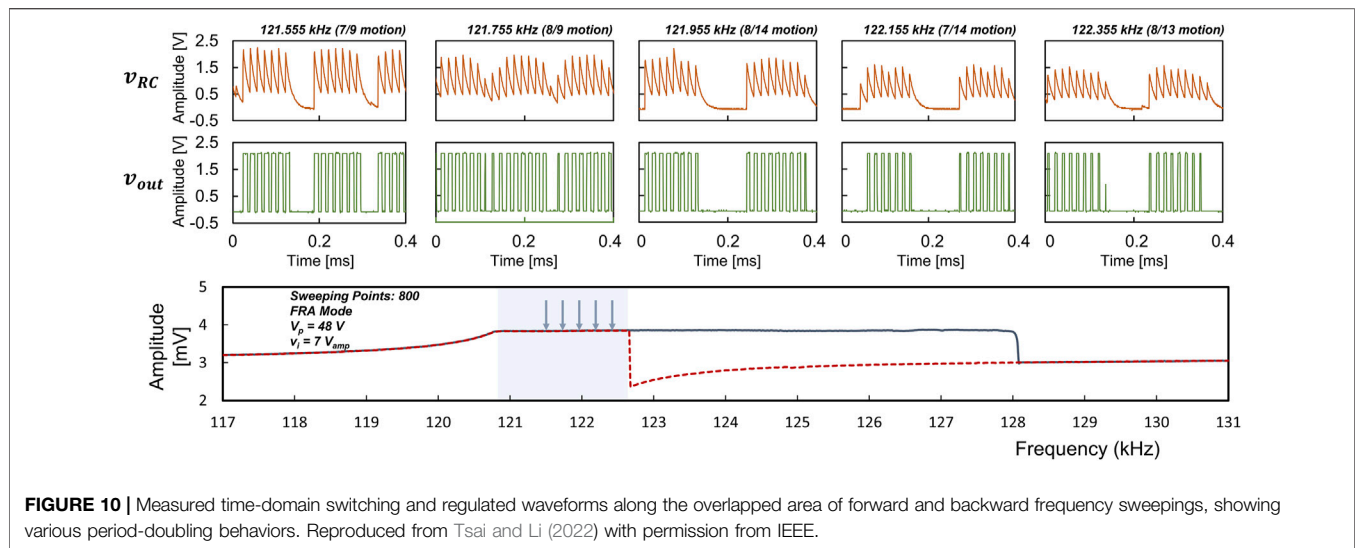
5.1 Frequency Stability

Nonlinear mechanical resonators have been shown to have better closed-loop frequency stability at the bifurcation points, where the amplitude frequency responses exhibit discontinuous transitions due to multiple amplitude states existing at one frequency (Yurke et al., 1995; Villanueva, 2013; Huang, 2019). This obviously applies to vibro-impact resonators, which would manifest bifurcations inherited from mechanical nonlinearity plus that due to impact. **Figure 8** plots the frequency response of a vibro-impact resonator, showing the displacement magnitude and phase. The tapping region occurs when the displacement is larger than the output gap spacing. Since the bifurcation yields multiple states in the magnitude for a given

FIGURE 10 | Measured time-domain switching and regulated waveforms along the overlapped area of forward and backward frequency sweepings, showing various period-doubling behaviors. Reproduced from Tsai and Li (2022) with permission from IEEE.

5.2 Clock Generators

In fact, the vibro-impact dynamic system could have even more complex behaviors in the time domain. Along the tapping region, the actual interaction between the structure and stoppers/electrodes would determine the time-domain responses—initial grazing, period doubling, chaotic, reverse period doubling, or saddle-node bifurcations. Tsai and Li (2022) reported the time-domain hot switching waveforms, similar to that in Tsai et al. (2020a) but with finer resolutions to see the variations along the tapping region. In particular, as shown in **Figure 10**, the five different input driving frequencies, one can obtain different pulse densities. This offers a pulse density modulation more flexible than that in Liu et al. (2017), which calls for mechanical structure modification. The bifurcation-induced pulse density modulation could also enable a more sophisticated modulation scheme other than the OOK or FSK used in Tsai et al. (2020a) for communication.

6 CONCLUSION AND FUTURE PERSPECTIVES

MEMS-based vibro-impact resonators enable a new class of resonant devices. In contrast to the traditional timing and frequency reference oriented counterparts, the vibro-impact resonators encompass impact-induced nonlinearity and in turn achieve many special devices with unique functions from resoswitches to on-chip surface monitoring to mechanical pulse width modulators. All of which is thanks to the CMOS-MEMS process platform used, which allows fast conceptual prototyping together with a promising path toward end products. To make the CMOS-MEMS platform prevail in the community, one would need to solve several challenges. To name a few, the process yield, electrical-mechanical coupling strength, resonator Q, and so on. For resoswitches in particular, the limited contact material choices lead to the need for structural design or post-fabrication processes to mitigate the issue. Abundant research possibilities accentuating this topic pave the way for future research activities.

AUTHOR CONTRIBUTIONS

C-PT and W-CL: substantial contributions to the conception of the work, analysis, and interpretation of published data for the work. All authors contributed to the article and approved the submitted version.

FUNDING

REFERENCES

Akgul, M. (2009). "Oscillator Far-From-Carrier Phase Noise Reduction via Nano-Scale Gap Tuning of Micromechanical Resonators," in the 15th International Conference. on Solid-State Sensors, Actuators, and Microsystems (TRANSDUCERS'09), Denver, CO, USA, 21–25 Jun, 798–801. doi:10.1109/sensor.2009.5285683

Atmel (2007). *Interface IC for 125 kHz Wake-Up Function: ATA5283 Datasheet.* San Jose: Atmel Corportation. [Online].

Austriamicrosystems (2015). *AS3932 3D Low Frequency Wakeup Receiver Datasheet.* Unterpremstaetten, Austria: ams AG. [Online].

Babitsky, V. I. (2013). *Theory of Vibro-Impact Systems and Applications* Berlin, Heidelberg: Springer.

Yang, W.-C. (2014). Broadband Vibrational Energy Harvesting Based on a Triboelectric Nanogenerator. *Adv. Energy Mater.* 4 (6), 1301322. doi:10. 1002/aenm.201301322

Chen, W.-C., Fang, W., and Li, S.-S. (2011). A Generalized CMOS-MEMS Platform for Micromechanical Resonators Monolithically Integrated with Circuits.

J. Micromech. Microeng., June. 21 (6), 5012. doi:10.1088/0960-1317/21/6/065012

Chen, W.-C., Fang, W., and Li, S.-S. (2012). High-Q Integrated CMOS-MEMS Resonators with Deep-Submicrometer Gaps and Quasi-Linear Frequency Tuning. *J. Microelectromechanical Syst.* 21 (3), 688–701. doi:10.1109/jmems.2012.2189360

Chiu, Y., Hong, H.-C., and Wu, P.-C. (2013). Development and Characterization of a CMOS-MEMS Accelerometer with Differential LC-Tank Oscillators. *J. Microelectromechanical Syst.* 22 (6), 1285–1295. doi:10.1109/jmems.2013.2282419

Dai, C.-L. (2006). A Maskless Wet Etching Silicon Dioxide Post-CMOS Process and its Application. *Microelectron. Eng.* 83 (11-12), 2543–2550. doi:10.1016/j.mee.2006.06.006

Dauksevicius, R. (2019). Nonlinear Piezoelectric Vibration Energy Harvester with Frequency-Tuned Impacting Resonators for Improving Broadband Performance at Low Frequencies. *Smart Mater. Struct. Jan.* 28 (2), 025025. doi:10.1088/1361-665x/aaf358

Derjaguin, B. V., Muller, V. M., and Toporov, Y. P. (1975). Effect of Contact Deformations on the Adhesion of Particles. *J. Colloid Interface Sci.* 53 (2), 314–326. doi:10.1016/0021-9797(75)90018-1

Fedder, G. K. (1996). Laminated High-Aspect-Ratio Microstructures in a Conventional CMOS Process. *Sensors Actuators A Phys.* 57 (2), 103–110. doi:10.1016/s0924-4247(97)80100-8

Fu, Y., Ouyang, H., and Davis, R. B. (2018). Nonlinear Dynamics and Triboelectric Energy Harvesting From a Three-Degree-of-Freedom Vibro-Impact Oscillator. *Nonlinear Dynamics*, 1985–2004. doi:10.1007/s11071-018-4176-3

Galanko, M. E. (2017). "CMOS-MEMS Resonant Demodulator for Near-Zero-Power RF Wake-Up Receiver," in the 19th International Conference on Solid-State Sensors, Actuators and Microsystems (TRANSDUCERS'17), Kaohsiung, Taiwan, 18–22 Jun, 86–89. doi:10.1109/transducers.2017.7993994

He, T., Lee, J., Wang, Z., and Feng, P. X.-L. (2014). "Interrogating Contact-Mode Silicon Carbide (SiC) Nanoelectromechanical Switching Dynamics by Ultrasensitive Laser Interferometry," in 2014 IEEE 27th International Conference on Micro Electro Mechanical Systems (MEMS), 1079–1082. doi:10.1109/memsys.2014.6765832

Hölscher, H. (2012). *AFM, Tapping Mode*. Encyclopedia of Nanotechnology.

Hsu, C.-E., and Li, W.-C. (2020). Mitigating the Insufficient Etching Selectivity in the Wet Release Process of CMOS-MEMS Metal Resonators via Diffusion Control. *J. Microelectromechanical Syst. Lett.* 29 (6), 1415–1417. doi:10.1109/jmems.2020.3028291

Huang, L. (2019). Frequency Stabilization and Noise-Induced Spectral Narrowing in Resonators with Zero Dispersion. *Nat. Commun.* 10 (1), 3930. doi:10.1038/s41467-019-11946-8

Kim, B. (2009). "Micromechanical Resonant Displacement Gain Stages," in the 22nd IEEE International Conference on Micro Electro Mechanical Systems (MEMS'09, Sorrento, Italy, 25–29 Jan, 2519–2922. doi:10.1109/memsys.2009.4805308

Lee, S. I., Howell, S. W., Raman, A., and Reifenberger, R. (2002). Nonlinear Dynamics of Microcantilevers in Tapping Mode Atomic Force Microscopy: A Comparison between Theory and Experiment. *Phys. Rev. B, Sep.* 66 (11), 115409. doi:10.1103/physrevb.66.115409

Lee, Y.-C. (2021a). "A CMOS-MEMS Fluorescence Quenching Gas Sensor Encapsulated with Silicon-Based LED Reflector," in 2021 21st International Conference on Solid-State Sensors, Actuators and Microsystems (TRANSDUCERS'21), Orlando, FL, USA, 20–24 Jun, 783–786. doi:10.1109/transducers50396.2021.9495443

Lee, Y.-C. (2021b). CMOS-MEMS Technologies for the Applications of Environment Sensors and Environment Sensing Hubs. *J. Micromechanics Microengineering, June* 31 (7), 074004. doi:10.1088/1361-6439/ac0514

Li, M.-H., Chen, C.-Y., Liu, C.-Y., and Li, S.-S. (2016). A Sub-150μW BEOL-Embedded CMOS-MEMS Oscillator with a 138dBΩ Ultra-low-noise TIA. *IEEE Electron Device Lett.* 37 (5), 648–651. doi:10.1109/led.2016.2538772

Li, W.-C., Lin, Y., and Nguyen, C. T.-C. (2013). "Metal Micromechanical Filter-Power Amplifier Utilizing A Displacement-Amplifying Resonant Switch," in 2013 Transducers and Eurosensors XXVII: The 17th International Conference on Solid-State Sensors, Actuators and Microsystems (TRANSDUCERS'13), Barcelona, Spain, 16–20 Jun, 2469–2472. doi:10.1109/transducers.2013.6627306

Li, W.-C., Ren, Z., and Nguyen, C. T.-C. (2016). "A Micromechanical High-Q Elliptic Disk Displacement Amplifier," in the 29th IEEE International Conference on Micro Electro Mechanical Systems (MEMS'16), Shanghai, China, 24–28 Jan, 663–666. doi:10.1109/memsys.2016.7421713

Liao, Y.-Y. (2019). *A CMOS-MEMS Folded-Beam Resoswitch-Based OOK/FSK Communication Receiver*. Taipei: Master ThesisNational Taiwan University.

Lin, Y. (2011). "A Metal Micromechanical Resonant Switch for On-Chip Power Applications," in Tech. Digest 2012 IEEE Int. Electron Devices Mtg. (IEDM'11), Washington, DC, 5–7 Dec, 162–165. doi:10.1109/iedm.2011.6131593

Lin, Y. (2009). "Digitally-specified Micromechanical Displacement Amplifiers," in 2009 International Solid-State Sensors, Actuators and Microsystems Conference (TRANSDUCER'09), Denver, CO, USA, 21–25 Jun, 781–784. doi:10.1109/sensor.2009.5285651

Lin, Y., Li, W.-C., and Nguyen, C. T.-C. (2013). "A MEMS-Based Charge Pump," in 2013 Symposium on VLSI Technology, Kyoto, Japan, 11–13 Jun, T148–T149.11-13 June

Lin, Y., Li, W.-C., Ren, Z., and Nguyen, C. T.-C., 2008. A Resonance Dynamical Approach to Faster, More Reliable Micromechanical Switches," in 2008 IEEE International Frequency Control Symposium, Honolulu, HI, 19–21 May, 640–645. doi:10.1109/freq.2008.4623078

Lin, Y., Liu, R., Li, W.-C., and Nguyen, C. T.-C. (2014). "Polycide Contact Interface to Suppress Squegging in Micromechanical Resoswitches," in 2014 IEEE 27th International Conference on Micro Electro Mechanical Systems (MEMS'14), San Francisco, CA, USA, 26–30 Jan, 261273–301276. doi:10.1109/memsys.2014.6765881

Liu, J.-R., Lu, S.-C., Tsai, C.-P., and Li, W.-C. (2018). A CMOS-MEMS Clamped–Clamped Beam Displacement Amplifier for Resonant Switch Applications. *J. Micromech. Microeng. (JMM)* 28 (6), 065001. doi:10.1088/1361-6439/aab112

Liu, R., Nilchi, J., Li, W.-C., and Nguyen, C. T.-C., (2016). Soft-impacting Micromechanical Resoswitch Zero-Quiescent Power AM Receiver," in The 29th IEEE International Conference on Micro Electro Mechanical Systems (MEMS'16), Shanghai, China, 24–28 Jan, 51–54. doi:10.1109/memsys.2016.7421555

Liu, R., Nilchi, J. N., and Nguyen, C. T.-C. (2017). "CW-powered Squegging Micromechanical Clock Generator," in 2017 IEEE 30th International Conference on Micro Electro Mechanical Systems (MEMS'17), Las Vegas, NV, USA, 22–26 Jan, 905–908. doi:10.1109/memsys.2017.7863555

Liu, R. (2015). "Zero Quiescent Power VLF Mechanical Communication Receiver," in 2015 18th International Conference on Solid-State Sensors, Actuators and Microsystems (TRANSDUCERS'15, Anchorage, AK, USA, 21–25 Jun, 51–54. doi:10.1109/transducers.2015.7180878

Liu, Y.-C. (2013). Temperature-Compensated CMOS-MEMS Oxide Resonators. *IEEE/ASME J. Microelectromech. Syst. (JMEMS)* 22 (5), 1054–1065. doi:10.1109/jmems.2013.2263091

Lo, C.-C., Chen, F., and Fedder, G. K. (2005). "Integrated HF CMOS-MEMS Square-Frame Resonators with On-Chip Electronics and Electrothermal Narrow Gap Mechanism,"in The 13th International Conference on Solid-State Sensors, Actuators and Microsystems, 2005. Digest of Technical Papers (TRANSDUCERS '05), Seoul, South Korea, 5–9 Jun, 2074–2077.

Lopez, J. L. (2009). Integration of RF-MEMS Resonators on Submicrometric Commercial CMOS Technologies. *J. Micromechanics Microengineering* 19 (1), 015002. doi:10.1088/0960-1317/19/1/015002

Lu, S.-C., Tsai, C.-P., and Li, W.-C. (2018a). "A CMOS-MEMS CC-Beam Metal Resoswitch for Zero Quiescent Power Receiver Applications," in Proc., 31st IEEE International Conference on Micro Electro Mechanical Systems (MEMS'18), Belfast, UK, 21–25 Jan, 801–804. doi:10.1109/memsys.2018.8346676

Lu, S.-C., Tsai, C.-P., and Carley, L. R. (2018b). Surface Condition Influence on the Nonlinear Response of MEMS CC-Beam Resoswitches. *IEEE Electron Device Lett.* 39 (10), 1600–1603. doi:10.1109/led.2018.2865956

Luo, A. C. J., and Guo, Y. (2013). *Vibro-impact Dynamics*. John Wiley and Sons.

Luo, H., Zhang, G., Carley, L. R., and Fedder, G. K. (2002). A Post-CMOS Micromachined Lateral Accelerometer. *J. Microelectromechanical Syst. June* 11 (3), 188–195. doi:10.1109/jmems.2002.1007397

Ma, Q. (2007). Metal Contact Reliability of RF MEMS Switches. *Proc. SPIE, Jan.* 6463, 646–305. doi:10.1117/12.702177

Marigo, E. (2010). Zero-level Packaging of MEMS in Standard CMOS Technology. *J. Micromechanics Microengineering* 20 (6), 064009. doi:10.1088/0960-1317/20/6/064009

Moss, S. (2010). A Low Profile Vibro-Impacting Energy Harvester with Symmetrical Stops. *Appl. Phys. Lett. Nov.* 97 (23), 234101. doi:10.1063/1.3521265

Patton, S., and Zabinski, J. (2005). Fundamental Studies of Au Contacts in MEMS RF Switches. *Tribol. Lett.* 18, 215–230. doi:10.1007/s11249-004-1778-3

Peschot, A. (2014). Evolution of Contact Bounces in MEMS Switches under atlCycling," in 2014 IEEE 60th Holm Conference on Electrical Contacts (Holm), New Orleans, LA, USA, 12–15 Oct, 1–6.

Pyatishev, E. (2017). "A Micromechanical Gyroscope with Bistable Suspension of Microdrive," in 2017 24th Saint Petersburg International Conference on Integrated Navigation Systems ICINS, St. Petersburg, Russia, 29–31 May, 29–31. doi:10.23919/icins.2017.7995646

Rhoads, J. F., Shaw, S. W., and Turner, K. L. (2010). Nonlinear Dynamics and its Applications in Micro- and Nanoresonators. *ASME. J. Dyn. Sys., Meas. Control* 132 (3), 034001. doi:10.1115/1.4001333

Riverola, M. (2016). A Monolithically Integrated Torsional CMOS-MEMS Relay. *J. Micromechanics Microengineering* 26, 115012. doi:10.1088/0960-1317/26/11/115012

Riverola, M., Uranga, A., Torres, F., and Barniol, N. (2018). Fabrication and Characterization of a Hammer-Shaped CMOS/BEOL-embedded Nanoelectromechanical (NEM) Relay. *Microelectron. Eng.* 192, 44–51. doi:10.1016/j.mee.2018.01.029

Riverola, M., Vidal-Alavez, G., and Sobreveila, V. (2016). Dynamic Properties of Three-Terminal Tungsten CMOS-NEM Relays under Nonlinear Tapping Mode. *IEEE Sensors J.* 16 (13), 5283–5291. doi:10.1109/jsen.2016.2561321

Riverola, M., Vidal-Alvarez, G., Torres, F., and Barniol, N. (2014). "3-terminal Tungsten CMOS-NEM Relay," in 2014 10th Conference on Ph.D. Research in Microelectronics and Electronics (PRIME), Grenoble, France, 30 Jun–3 Jul. doi:10.1109/prime.2014.6872734

Sun, C.-M., Tsai, M.-H., and Fang, W. (2010). Implementation of a Monolithic Single Proof-Mass Tri-axis Accelerometer Using CMOS-MEMS Technique. *IEEE Trans. Electron devices* 57 (7), 1670–1679. doi:10.1109/ted.2010.2048791

Tsai, C.-P., and Li, W.-C. (2022). "A Micromechanical Frequency Controlled Pulse Density Modulator," in the 35th IEEE Int. Conference on Micro Electro Mechanical Systems (MEMS'22), Tokyo, Japan, 9-13 Jan, 204–207. doi:10.1109/mems51670.2022.9699549

Tsai, C.-P., Liao, Y.-Y., and Li, W.-C. (2020a). "A 125-kHz CMOS-MEMS Resoswitch Embedded Zero Quiescent Power OOK/FSK Receiver," in 33rd IEEE Int. Conference on Micro Electro Mechanical Systems (MEMS'20), Vancouver, BC, Canada, 18–22 Jan, 106–109. doi:10.1109/mems46641.2020.9056120

Tsai, C.-P., Liu, J.-R., and Li, W.-C. (2020b). Experimental Study on Frequency Stability of Micromechanical Resonators Operating in the Nonlinear Tapping Mode," in Proc., 2020 IEEE Int. Frequency Control Symposium (IFCS'20), Keystone, CO, USA, 19–23 Jul. doi:10.1109/ifcs-isaf41089.2020.9234814

Verd, J. (2005). Design, Fabrication, and Characterization of a Submicroelectromechanical Resonator with Monolithically Integrated CMOS

Readout Circuit. *J. Micro. Electro. Mechanical Syst.*, 508–519. doi:10.1109/jmems.2005.844845

Verd, J. (2008). Monolithic CMOS MEMS Oscillator Circuit for Sensing in the Attogram Range. *IEEE Electron Device Lett.* 29 (2), 146–148. doi:10.1109/led.2007.914085

Villanueva, L. G. (2013). Surpassing Fundamental Limits of Oscillators Using Nonlinear Resonators. *Phys. Rev. Lett.* 110 (17), 177208. doi:10.1103/physrevlett.110.177208

Wu, J., Fedder, G. K., and Carley, L. R. (2004). A Low-Noise Low-Offset Capacitive Sensing Amplifier for a 50-ug/sqrt(Hz) Monolithic CMOS MEMS Accelerometer. *IEEE J. Solid-State Circuits* 39 (5), 722–730. doi:10.1109/jssc.2004.826329

Wu, T. (2017). "A Microelectromechanical AlN Resoswitch for RF Receiver Application," in the 19th Int. Conf. on Solid-State Sensors, Actuators, and Microsystems (TRANSDUCERS'17), Kaohsiung, Taiwan, 18–22 Jun, 2123–2126. doi:10.1109/transducers.2017.7994494

Xie, H., and Fedder, G. K. (2003). Fabrication, Characterization, and Analysis of a DRIE CMOS-MEMS Gyroscope. *IEEE Sensors J.* 3 (5), 622–631. doi:10.1109/jsen.2003.817901

Xu, W. (2016). Theoretical and Experimental Investigations of Thermoresistive Micro Calorimetric Flow Sensors Fabricated by CMOS MEMS Technology. *J. Microelectromechanical Syst.* 25 (5), 954–962. doi:10.1109/jmems.2016.2596282

Yurke, B., Greywall, D. S., Pargellis, A. N., and Busch, P. A. (1995). Theory of Amplifier-Noise Evasion in an Oscillator Employing a Nonlinear Resonator. *Phys. Rev. A* 51 (5), 4211–4229. doi:10.1103/physreva.51.4211

Zhang, W., Zhang, W., and Turner, K. L. (2005). "Nonlinear Dynamics of Micro Impact Oscillators in High Frequency MEMS Switch Application," in The 13th International Conference on Solid-State Sensors, Actuators and Microsystems (TRANSDUCERS'05), Seoul, South Korea, 5–9 Jun, 768–771.

Zheng, H.-S., Tsai, C.-P., Chen, T.-Y., and Li, W.-C. (2022). "CMOS-MEMS Resonators with Sub-100-nm Transducer Gap Using Stress Engineering," in The 35th IEEE International Conference on Micro Electro Mechanical Systems (MEMS'22), Tokyo, Japan, 9–13 Jan, 13–16. doi:10.1109/mems51670.2022.9699732